Modeling the underwater electromagnetic radio frequency channel in the DESERT Underwater network simulator

Riccardo Tumiati, Filippo Campagnaro, Irene Cappelli, Alessandro Pozzebon, Michele Zorzi

***Abstract*—The possibility of transmitting data in fresh water scenarios using Low-Rate Long Range (LoRa) wireless sensors may enable in the near future new applications, such as wireless sensor deployments for monitoring quay walls, river pillars, and any type of infrastructure and platform deployed in rivers and lakes. In fact, while in salt water this technology has a transmission range of only a few centimeters, making acoustic modems more suitable for this scenario, in fresh water it can cover a range of a couple of meters with standard very low power devices [1]. Another advantage of this technology is the possibility to cross the water-to-air boundary, enabling the communication between underwater and surface devices. The electromagnetic propagation in this scenario has been analyzed in [1], where the authors validated their analytical model thanks to an extensive set of field measurements performed in a swimming pool. This model has been implemented in the DESERT Underwater simulation and experimentation framework to simulate radio frequency underwater network deployments. In this paper we discuss this model and how it was integrated in DESERT, showing a potential application of an underwater LoRa network deployment measuring the network performance via simulations.**

***Index Terms*—Underwater networks, underwater internet of things, LoRa, channel models, simulation, field measurements, DESERT Underwater, transmission performances**

I. Introduction

The underwater environment is one of the most challenging communication scenarios, due to the intrinsic properties of the underwater channel, characterized by strong attenuation of Radio Frequency (RF) Electromagnetic (EM) waves (especially in salt water), and high variability of the transmission conditions in both time and space, due to changes of temperature, salinity, density and pressure along the water column, and to the presence of waves and tides that cause variation of the water level in the short and medium time. Moreover, crossing the water-to-air interface causes a severe degradation of the signal, which is also strongly reflected by the seafloor and the water surface. For this reason the most common transmission methods in the open sea are acoustic [2] and optical [3] communications, with the former able to reach several kilometers with low-rate communication links, and the latter capable of broadband short-range transmissions. Nevertheless, in the last years, there has been some re-evaluation of the RF EM waves to perform communication under water [1], [4], [5]. In fact, RF waves are less affected by phenomena like Doppler, multipath, shipping noise, water turbidity and sunlight noise, factors that cause the degradation of either acoustic or optical communication links [6], and are the only technology able to cross the water-to-air boundary and reach an external device not immersed in the sea (e.g., a Gateway). Moreover, RF transceivers are orders of magnitude cheaper than acoustic and optical modems. The main problems related to RF are the high attenuation of the signal and the propagation difficulties. Furthermore, there are problems related to the floor refractions of lakes, seas and rivers. However, the viability of establishing an underwater radio link was extensively proven in the last century, in both salt and fresh water, but the applications were limited to the Extremely Low Frequency (ELF) and the Very Low Frequency (VLF) ranges [7], [8], which made possible the coverage of very long distances (i.e., up to several kilometers) but at the cost of large antennas, low data rates and high transmitting power. As a consequence, solutions involving low frequency technologies are not suitable for dense and distributed Underwater Wireless Sensor Networks (UWSNs). Moving to higher frequencies, the reliability of the transmission can be compromised by the higher electromagnetic attenuation experienced during wave propagation. However, several scientific contributions report applications involving Low Frequency (LF) [9], [10], High Frequency (HF) [11], [12] and Ultra High Frequency (UHF) [13], [14] radio channels, with promising results: short-range communication links (approximately 2 m) are achieved, which can be a sufficient radio coverage for the development of UWSNs for the monitoring of submerged infrastructures in rivers and lakes. In particular, the UHF range is one of the most promising for the development of underwater sensor networks in critical scenarios, since many of the novel transmission technologies that faced the market in the last decade for the wireless sensor network framework (like SigFox, NB-IoT, ZigBee and Long-Range Low Rate (LoRa)) operate in this range.

In this paper we model in the DESERT Underwater network simulator [15] the propagation of the underwater EM channel and simulate RF transmissions in a flexible underwater net-

R. Tumiati (email: riccardo.tumiati@studenti.unipd.it), F. Campagnaro (email: campagn1@dei.unipd.it), A. Pozzebon (email: alessandro.pozzebon@unipd.it), and M. Zorzi (email: zorzi@dei.unipd.it) are with the Department of Information Engineering, University of Padova, Italy, I. Cappelli (email: cappelli@diism.unisi.it) is with the Department of Information Engineering and Mathematics, University of Siena, Italy.

This work has been partially supported by the European Union under the Italian National Recovery and Resilience Plan (NRRP) of NextGenerationEU, partnership on "Telecommunications of the Future" (PE0000001 - program "RESTART"), the National Biodiversity Future Center (NBFC), PNRR, CN00000033, Spoke 1, and the FSE REACT EU, PON Research and Innovation 2014-2020 (DM 1062/2021).

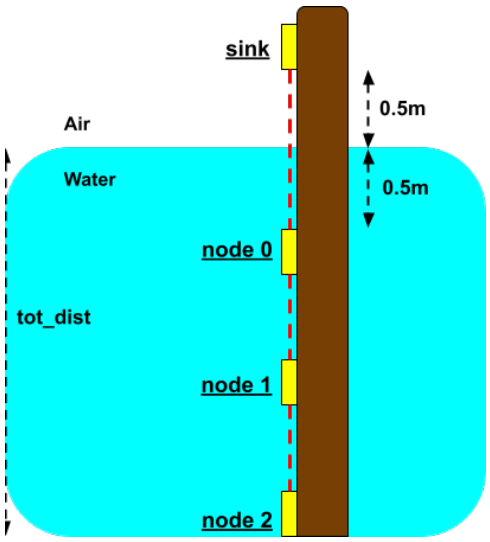

Fig. 1: Communication scenario

work scenario. The starting point for the development is the study performed in [1], where the EM channel is extensively analyzed and the proposed model is compared with real field measurements performed in a fresh water swimming pool. Specifically, in [1] LoRa [16], one of the most popular Sub-GHz technologies (LoRa uses a carrier frequency of 868 MHz in Europe and of 915 MHz in the US), has been analyzed because it achieves a significantly long range with low power consumption. Nevertheless, this model can be extended to other RF technologies as well, without loss of generality. In [1] the reference scenario was a Point-to-point (P2P) Underwater-to-above water (UW2AW) communication between two nodes, one immersed in the pool and one out of the water. The authors both computed the Received Signal Strenght Indicator (RSSI), adapting the theoretical model in [17], and testing it experimentally, also measuring the associated Packet Loss (PL) probability, compiling tables of RSSI-PL pairs. In this paper we include this model in a complete network simulator to evaluate a complete network deployment composed by multiple nodes deployed under and above water with a large range of flexibility in terms of configuration, from the number and the position of the nodes, to the water characteristics and the protocol stack used by the nodes. In addition, we simulate a possible specific real field scenario composed of several nodes deployed along a river pier, aiming to convey their data to a surface sink (Figure 1). This is a more complex situation than the original experiment, because of the greater number of nodes (more hops) and the combination of Underwater-to-underwater (UW2UW) and UW2AW communications.

To perform the simulations, we extended the DESERT Underwater framework [15], an underwater network simulation and experimentation tool developed in C++ that implements several models and protocols for underwater acoustic and optical networks, including three new modules to simulate underwater RF transmissions, namely: `uwem-channel` that simulates the channel, `uwem-mpropagation` that simulates the EM path loss, and `uwem-phy` that simulates the physical layer and computes the Packet Error Rate (PER). Specifically, `uwem-channel` forwards the packet from the transmitter to the receiver computing the propagation delay in water, `uwem-phy` computes the RSSI considering the transmission power and the path loss computed by `uwem-mpropagation` with the mathematical model presented in [1] and [17], where the attenuation of the signal is computed analytically starting from the temperature, the carrier frequency, the salinity of the water and the distance between transmitter and receiver. Then, `uwem-phy` maps the RSSI to the corresponding PER obtained with the measurements performed in [1] and included in the simulator in the form of Lookup Tables (LUTs). Note that LUTs depend on a set of communication parameters established in advance: Code Rate (CR), Spreading Factor (SF) and Bandwidth (BW).

The paper is structured as follows. Section II describes widely the new modules introduced in DESERT, `uwem-channel`, `uwem-mpropagation`, and `uwem-phy`, showing how the empirical model is developed practically. Then, Section III describes the considered scenario and the simulation parameters. Section IV discusses the simulation results and the statistical analysis of the observed Key Performance Indicators (KPIs). Moreover, it evaluates the optimal distance between nodes to carry the data from the bottom of the river to the water surface, examining different water depths, from 10 m to 200 m, and the number of retransmissions needed to ensure a packet delivery ratio of at least 90%.

Finally, Section V concludes this paper and discusses future developments.

II. Electromagnetic transmission simulator

The EM channel and RF transmissions in general have always been scarcely considered for the underwater environment, due to their short range. However, their potential use in a fresh water environment deserves more investigation and analysis of possible use-cases at least in simulation. Originally, DESERT supported simulations of only underwater acoustic and optical networks, hence there was the need to expand the framework with new modules for simulating underwater RF transmissions. In the DESERT Underwater Framework structure, in order to simulate a new type of communication technology, three different software components, called modules, need to be developed: the channel, propagation and physical layer modules. In the next sub-sections we are going to describe the new functionalities introduced in the simulator for each of the new components (`uwem-channel`, `uwem-mpropagation` and `uwem-phy`).

A. Channel

The channel module, named `uwem-channel`, is an abstraction of the physical communication medium, which, in our case, is a wireless electromagnetic channel over the water. Every device must connect its physical layer module with it in order to be able to trace the packets that are sent through.

This module has two main functionalities, i.e., to:

- calculate the propagation delay depending on the distance from the source device to the receiving device;
- send up the packets to the physical layer of each node connected to the channel.

Since we are transmitting data via EM waves, they travel at the speed of light, that underwater is $2.26 \cdot 10^8$ m/s. The propagation delay can be easily calculated with the formula:

$$PropDelay = \frac{Distance}{SpeedOfLight} \tag{1}$$

B. Propagation

The aim of the propagation module, named `uwem-mpropagation`, is to elaborate analytically the attenuation of the communication depending on the parameters of the simulation. Following the procedure explained in [17], we can derive analytically the expression of the attenuation that depends on temperature, carrier frequency, salinity of the water and distance between transmitter and receiver. Moreover, with EM transmissions, we can cross the water-to-air boundary and therefore reach a sensor located above the water. The final complete attenuation equation, where each component is mathematically computed as presented in [1] is:

$$PL_{tot} = PL_{aw} + PL_{uw2aw} + PL_{uw} + L_m, \tag{2}$$

where PL_{aw} is the free space path loss for the above water path, PL_{uw2aw} is the attenuation of the water-air interface, PL_{uw} is the underwater path loss and finally, L_m accounts for miscellaneous losses, and is assumed equal to 0 in our model. This formula is used for UW2AW communications, so the path of our waves includes both the air and water parts. In case of UW2UW communications the first two terms (PL_{aw} and PL_{uw2aw}) are equal to 0, leaving only the single PL_{uw} attenuation term. The analytical formulation of these factors is fully described in [17].

The propagation model implements this path loss formula, which is used in the physical layer to determine the final RSSI.

C. Physical layer

Similarly to all the existing physical layer models in the DESERT Underwater framework, `uwem-phy` deals with sensing the communication channel in order to receive the packets that have been sent by a transmitting node. `Uwem-phy` works in this way: when a packet starts to be received by a node, the physical layer of that node calculates the RSSI of the signal using the link budget equation:

$$RSSI = P_t + G_t + G_r - PL_{tot}, \tag{3}$$

where P_t is the transmission power in dBm, G_t is the transmitter antenna gain in dBi, G_r is the receiver antenna gain in dBi and PL_{tot} is the path loss value obtained from the propagation model in Eq. (2).

If either the RSSI is less than a prefixed threshold (i.e., the receiver sensitivity) or the node is in the process of receiving another packet, this packet is dropped.

Afterwards, as soon as the packet reception finishes, the simulator computes the PL probability observing some radio parameters of the received signal (specified in the simulation): SF, CR, and BW. Knowing them, it opens the corresponding LUT present in the DESERT library, which specifies pairs of RSSI - PL for the specific communication case. These LUTs are obtained empirically from a real simulation environment, as explained in [1].

With the computed RSSI, `uwem-phy` performs an interpolation using the LUT data, deriving the PL used in a uniform random error process to establish whether the packet is dropped or not. The two extremes of the LUT table are particular cases: if we obtain an RSSI value which is greater than the greatest limit in the LUT we will use its PL corresponding value (we can not achieve better performance as 0 error probability is too idealistic); conversely, if we compute an RSSI smaller than the smallest in the table we will set PL equal to 100% (all packets are dropped). Finally, if the packet is not dropped, it is sent up in the protocol stack.

III. Simulation scenario and node structure

TABLE I: Parameters properties: notation and meaning

Notation	Meaning	Value
Pkt	Packet size	25 B
T_{CBR}	CBR period	180 s
T	Simulation period	10000 s
f	Carrier frequency	868 MHz
B	Bandwidth	125 kHz
R	Physical bit-rate	5470 bit/s
$Temp$	Temperature of the water	20°C
S	Salinity of the water	0 $(g/kg)^2$
G	Antenna gain	2 dBi
P_{tx}	Transmitting power	14 dBm
CR	Coding rate	4/5
SF	Spreading factor	7
c	Speed of light	$2.26 \cdot 10^8$ m/s
w	CSMA wait constant	0.04 s
l	CSMA listen time	0.0001 s
N	Number of intermediate nodes (sink excluded)	Variable
n	Index of the node	0:$(N-1)$
d	Total communication distance	Variable
N_{RTX}	Max. number of retransmissions at layer 2	0:2

TABLE II: LUT table for SF 7, B = 125 kHz, CR = 4/5

RSSI (dBm)	PL%
$<$ - 109.45	100
- 109.45	6.5
- 97.75	2.5
$>$ - 97.75	2.5

With the simulator completely developed, the next step of this project was to perform some simulations in a realistic case, observing results, making some statistical analysis and obtaining some insights. In the considered scenario, we envision the deployment of an underwater sensor network for

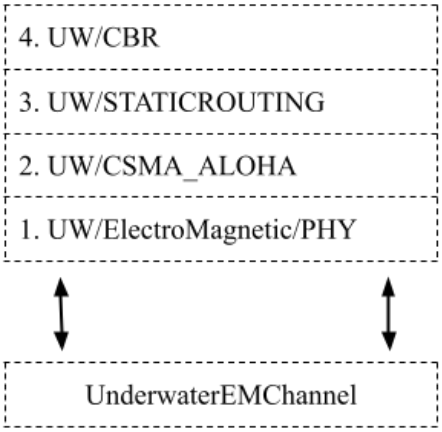

Fig. 2: Protocol stack used in the simulations

collecting various water measurements, such as temperature, density, and salinity, at different depths. In a real environment, this could be realized setting a certain number of sensors in the pillars of a bridge, or in general in any pillar that is immersed in the water. A schematic sketch of the envisioned scenario is shown in Figure 1; in the simulations we considered different numbers of intermediate nodes N (not only four as shown in the figure) and a total depth to be reached d.

The sink, placed outside the water at the fixed height of 0.5 m, is a node collecting all the data packets arriving from the submerged sensors and forwarding them to a shore server (e.g., with an above water RF connection). Under the water, there is a variable number of nodes N that are sensing the environment, each transmitting its data (and forwarding the data received from the node below) via RF to the node above. While node 0, i.e., the closest node to the sink, is placed at a fixed depth of 0.5 m to allow the transmission to cross the water-to-air boundary in the optimal manner, the other nodes are placed one on top of the other, equally spaced with a distance proportional to the total maximum depth we want to reach. The number of nodes and the maximum depth are varied in the simulations. The maximum range for one hop communication is almost two meters, where the RSSI is approximately -120 dBm.

Every node in the network must deal with two specific tasks: (i) send its new data collected by the sensors, and (ii) forward the packets arriving from the bottom node, therefore the closer a node is to the sink the more packets it has to forward. All nodes use the same protocol stack (Figure 2): a constant bitrate (CBR) application layer, that generates traffic on average with a constant rate, static routing, as each node needs to forward its packets to its one-hop neighbor on top, Carrier-Sense Multiple Access (CSMA) Medium Access Control (MAC) and, finally, the underwater electromagnetic physical layer. From a network perspective, routing tables contain just one row, with the sink destination IP and the next hop set to the IP of the node on top of the current one. All the CBR flows are directed towards the sink with a fixed data generation rate corresponding to the ratio between the packet size and the CBR period, Pkt /

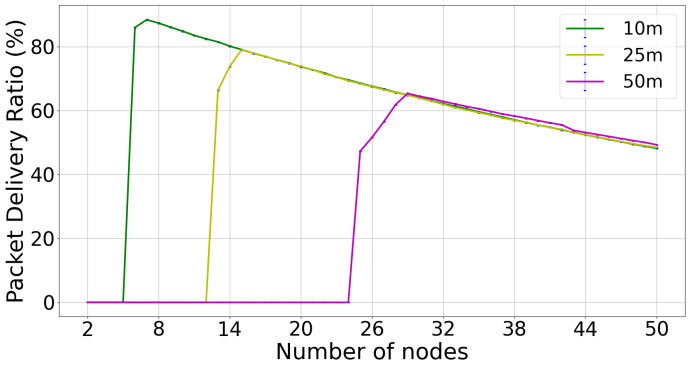

Fig. 3: Packet Delivery Ratio versus number of intermediate nodes N

T_{CBR} = 1.11 bps (T_{CBR} = 180 s). Although the single hop communication range is limited by the channel to no more than 2 meters, with the node displacement presented in Figure 1 we can reach very high depths, at the cost of lower throughput and packet delivery ratio.

Table I lists the most significant parameters used in our simulation, including physical properties and protocol settings. The two CSMA times (l and w) have been set according to some preliminary tests in order to avoid as much as possible collisions between packets in the stations. For completeness, w is a fixed minimum constant time a station listens to the channel before transmitting. In addition, a uniform random time with maximum value l is added. At the end of the listening phase, if the channel is idle the node can finally send the packet. In Table II we report the LUT used in our scenario; this is an exact copy of what has been measured in the real field [1].

IV. Simulation Results and Statistical Analysis

A. Optimal distance between two nodes

TABLE III: Maximum Packet Delivery Ratio (PDR) values without retransmissions

d	*N*	Node distance	PDR Mean	PDR Std	PDR CI 95%
10 m	7	1.583 m	88.393742	0.999363	0.195875
25 m	15	1.75 m	79.014365	0.767603	0.15045
50 m	29	1.767 m	65.349589	0.782051	0.153282

The first thing we want to investigate is the optimal distance between two nodes in order to achieve the best performance in terms of PDR and also to understand whether this value is constant or is depth dependent. We tested three network configurations (d = 10 m, d = 25 m, d = 50 m) varying the total number of sensors N to cover the distance from 2 up to 50 nodes (including the closest node to the surface). Increasing N means decreasing the distance between adjacent nodes since we are covering the same total depth with more nodes. For each pair d-N we performed 100 simulation runs observing the average KPIs. Specifically, on the sink side we observed: mean throughput (computed summing the number of bits that the sink has received during the simulation divided by the total

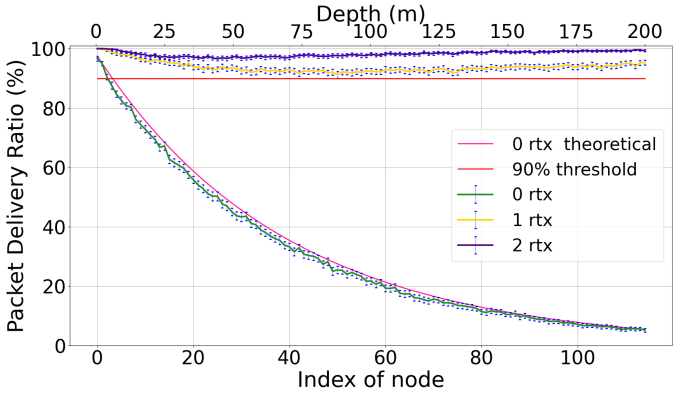

Fig. 4: Packet Delivery Ratio versus index of the node n

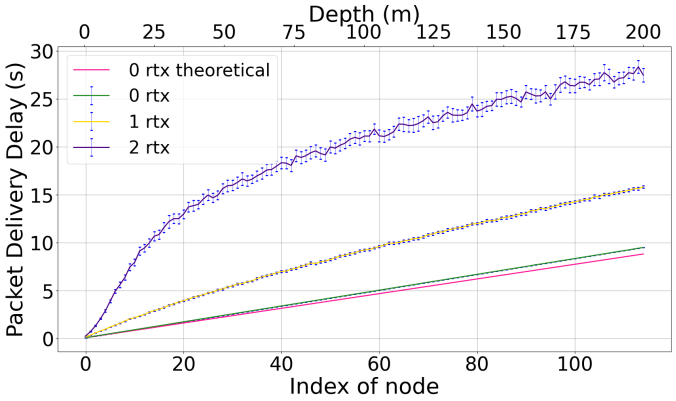

Fig. 5: Packet Delivery Delay versus index of the node n

simulation time), mean PDR (ratio between received packets and sent packets) and mean Packet Delivery Delay (PDD). The term mean is used to indicate an average with respect to the values obtained by all the nodes. For each of them, in turn we computed the mean value over the 100 runs, the standard deviation and the 95% confidence intervals for the mean. For this initial task we were interested only in the PDR metric, plotted in Figure 3. 95% confidence intervals of the mean are estimated using the general theorem for iid random variables:

$$\hat{\mu} \pm \eta \frac{std}{\sqrt{RUN}} \tag{4}$$

where η = 1.96 for 95% CI and RUN = 100, number of runs.

For these initial simulations retransmission systems have not been used in layer 2 nor in layer 3, which implies that the single packet can be received correctly by the sink if and only if the transmission is successful for each hop. Furthermore, only for this case, we generated traffic by all the immersed nodes excluding the first one, whose position is fixed at 0.5 m depth and does not change as a function of the total number of nodes. Observing the three curves we can spot that they have a visible maximum point which corresponds to the highest PDR achievable for a certain distance with a specific number of nodes. These three values are shown in Table III, which reports also the corresponding node distances computed as (D-0.5)/(N-1). It is clear that there is a fixed node distance where the trade-off error per single link, joint error probability (after multi-hop process) and probability of collision are minimized, and this value is about 1.75 m. After fixing this value, we measured the corresponding PL for the single link, which was found simply equal to 0.025 (2.5%). Observing Table II this is the smallest value achievable in a range of RSSI from 0 dBm to -97.75 dBm. This is an important conclusion that will be used in the next paragraph. In a real field environment it is difficult to deploy the sensor with a centimeter precision, but we can assert that if the distance between adjacent node ranges between 1.6 m and 1.77 m we are very close to the optimal deployment.

B. 200 meter depth scenario

After having obtained the optimal distance between two subsequent nodes we focused on an extreme scenario of 200

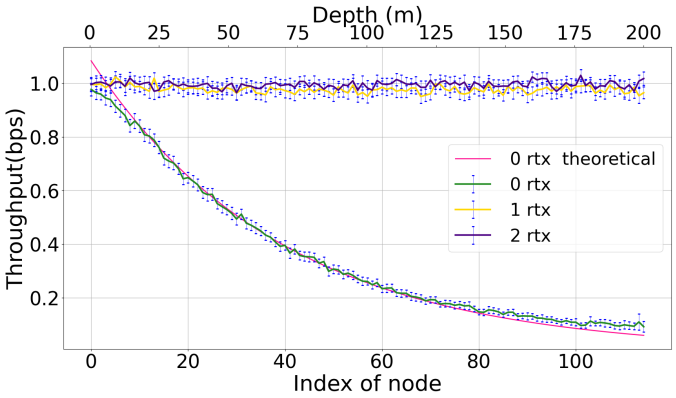

Fig. 6: Throughput versus index of the node n

meters depth. Probably this is an unrealistic case but it allows us to see how the performance is affected by the use of retransmissions. We set up the environment with d = 200 m, N = ((d - 0.5) / 1.75) + 1 = 115, N_{RTX} = 0,1,2, and all the other parameters the same as before. Our idea was to find the minimum N_{RTX} in order to satisfy a minimum performance threshold, that in our imaginary scenario was fixed as PDR greater than or equal to 90%, also for the worst case node. To achieve this result we ran 100 times the simulation for each value of N_{RTX} and observed the degradation of the performance going down to the deepest node. The worst case among all the set of nodes is not always the deepest one but it depends on the simulation run.

We measured the three KPIs in each node, we computed mean values among the 100 runs and confidence intervals and finally we plotted the results in Figure 4, Figure 5 and Figure 6. The x-axis presents both the index of the node and the corresponding depth, while the y axis of each figure shows a different performance indicator. For the PDR case we printed also the 90% threshold with a horizontal red line, highlighting the curves which satisfy the performance requirements. Then we computed the mean of the KPI previously measured in each node obtaining average statistics for the system, shown in Figure 7, Figure 8 and Figure 9. Also in this case the threshold line has been drawn in the PDR bar plot.

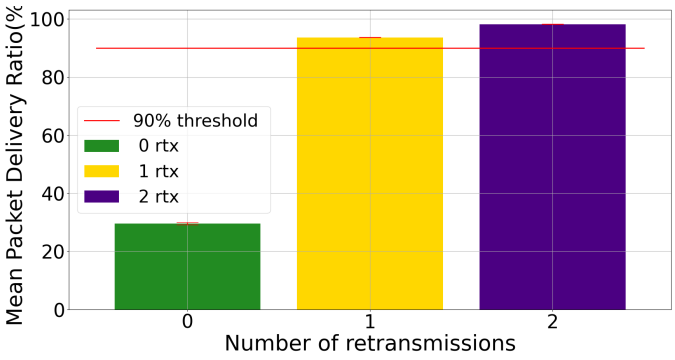

Fig. 7: Packet Delivery Ratio versus index of the node n

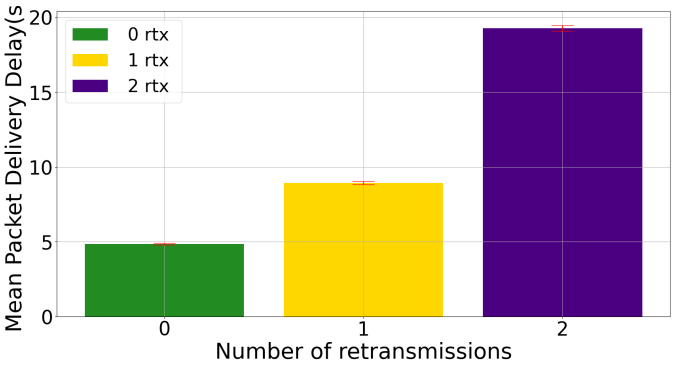

Fig. 8: Packet Delivery Delay versus index of the node n

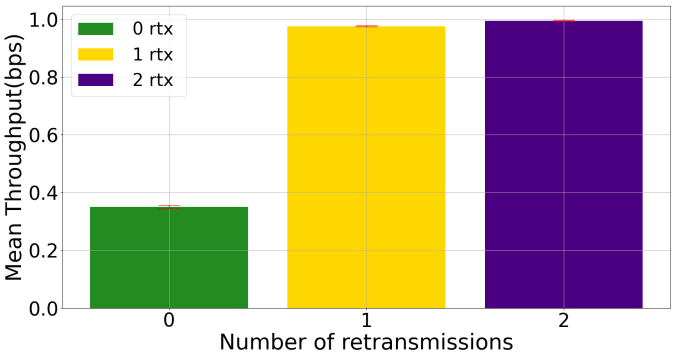

Fig. 9: Throughput versus index of the node n

It is easy to observe what is happening in terms of PDR in case of no retransmissions: the PDR decreases with respect to the index of the node and this is because the single link packet loss probability (PL) remains the same but the number of hops that the packet must travel in order to reach the sink increases (which results in a much more random experiment). In this case we cannot guarantee performance values which exceed the 90% threshold for all nodes but only for the those near the sink. Setting N_{RTX} equal to 1 and 2 we can satisfy the requirements for all the nodes in the chain. Note that increasing N_{RTX} means decreasing the single hop error probability but also increasing the congestion of the network. Now the question is: is it worth setting a maximum of 2 retransmissions for a slight increase of the PDR or is it better to set N_{RTX} to 1?

To answer this question we focused on the throughput and PDD plots. In the first one we can spot a little advantage also in this case for the 2 retransmission (RTX) case, comparable to that already seen in the PDR. We can see that the measured throughput is just a bit lower than the data generation, hence the nodes throughput with N_{RTX} = 2 is almost the maximum achievable in this network (and 5% higher than the one achievable with N_{RTX} = 1). However, the behavior of the PDD leads us to a different conclusion: the delay obtained with 2 RTXs is on average 3 times higher than the one observed with 1 RTX. In conclusion we can conclude that the 5% improvement of PDR and throughput does not justify the use of 2 RTXs as the resulting PDD is not acceptable, making the choice of 1 RTX the most suitable in our scenario.

C. Theoretical analysis of the no-retransmission case

In the above Figures 4, 5, 6, we also plotted the theoretical curves of the three KPIs for the case without retransmissions. This is a special predictable scenario where the behavior of the system can be easily derived from basic mathematical and probabilistic notions: this analysis, although somewhat redundant, proves that the simulated results are in line with what expected from the theory.

Specifically, we have first analyzed the PDR with respect to the index of the node i. Knowing the single hop PL probability (0.025) and the number of hops needed to reach the sink (i + 1), the expression of the final PDR can be expressed as:

$$PDR = 100 * (1 - PL)^{i+1}. \quad (5)$$

Analyzing the so obtained theoretical curve, in Figure 4 we can observe that it almost matches the curve obtained via simulation. Actually, the theoretical curve is a little more optimistic as it does not consider packet collisions. The throughput can be obtained from the product of the PDR with the data generation rate ($D_r = Pkt/T_{CBR}$ = 1.11 bps): similarly to the PDR, also for the throughput the theoretical curve matches the simulated one.

Finally, we computed the PDD, that is linearly growing with i. It depends on the propagation delay ($\tau = 1.75/c = 7.74 * 10^{-9}$ s), the transmission time ($T_{tran} = Pkt * 8/R = 0.0365$ s), the random time spent in queue (T_{queue}) and finally the listen time of the CSMA (T_l), which is a uniform random variable with mean $E[T_l] = w + (l/2) = 0.04005$ s. Since the network traffic is very low, we assume T_{queue} = 0 s. Given that T_l is not deterministic, we use its expectation to derive the theoretical PDD formula as follows:

$$PDD = (i + 1) * (\tau + T_{tran} + E[T_l] + T_{queue}). \quad (6)$$

Also in this case, as we can see in Figure 5, there is a small discrepancy between the theoretical PDD and the simulated one, due to T_{queue}, that we assumed to be 0 in our formula: the effect of T_{queue} is indeed negligible for the nodes close to the sink, but it accumulates as we move far from it. For the

deepest node it causes an additional delay of about 0.678 s (about 7% more).

V. Conclusions and future developments

In this paper we added to the DESERT Underwater framework the ability to simulate the underwater electromagnetic channel. The implemented propagation model was taken from [17]: this model was validated through extensive tests in [1] that measured the packet loss experienced with a certain RSSI, transmitting LoRa radio signals: these measurements have been included in DESERT in the form of LUTs. The implementation of this model in a network simulator allows us to test the feasibility of EM underwater network deployments and optimize the protocol stack: for instance, in this paper we envisioned a scenario where sensor nodes are deployed in a linear topology along a bridge pillar and want to transmit their data to a surface sink. First, we evaluated the trade-off between the number of devices and the distance to cover. Then, we investigated the number of retransmissions N_{RTX} per packet at the MAC layer to ensure a PDR of at least 90% for all the 115 nodes required to cover a depth of 200 m. Surprisingly, although without retransmissions the deepest node (that is the most disadvantaged) has a PDR of about 5%, with only one retransmission at the MAC it could achieve a PDR higher than 90%. A higher number of retransmissions is not desirable, because even though it will result in a higher PDR, it will also increase dramatically the PDD.

Future work will focus on refining the EM model, also including other important factors that can cause the signal degradation, such as noise and multipath. Experimental tests of a multihop underwater radio network in fresh water will also be performed in the near future.

References

[1] I. Cappelli, A. Fort, M. Mugnaini, S. Parrino, and A. Pozzebon, "Underwater to above water LoRaWAN networking: Theoretical analysis and field tests," *Measurement*, vol. 196, p. 111140, Jun. 2022.

[2] H. S. Dol, P. Casari, T. van der Zwan, and R. Otnes, "Software-Defined Underwater Acoustic Modems: Historical Review and the NILUS Approach," *IEEE Journal of Oceanic Engineering*, vol. 42, no. 3, pp. 722–737, Jul. 2017.

[3] Z. Zeng, S. Fu, H. Zhang, Y. Dong, and J. Cheng, "A Survey of Underwater Optical Wireless Communications," *IEEE Communications Survey and Tutorials*, vol. 19, no. 1, pp. 204–238, Firstquarter 2017.

[4] S. I. Inacio, M. R. Pereira, H. M. Santos, L. M. Pessoa, F. B. Teixeira, M. J. Lopes, O. Aboderin, and H. M. Salgado, "Dipole antenna for underwater radio communications," in *Proc. UComms, Lerici, Italy*, Aug. 2016.

[5] G. Ardelt, M. Mackenberg, J. Markmann, T. Esemann, and H. Hellbruck, "A flexible and modular platform for development of short-range underwater communication," in *Proc. ACM WUWNet, Shangai, China*, Oct. 2016.

[6] A. Pal, F. Campagnaro, K. Ashraf, M. R. Rahman, A. Ashok, and H. Guo, "Communication for underwater sensor networks: A comprehensive summary," *ACM Transactions on Sensor Networks*, vol. 19, no. 1, pp. 1–44, Dec 2022. [Online]. Available: https://doi.org/10.1145/3546827

[7] X. Che, I. Wells, G. Dickers, P. Kear, and X. Gong, "Re-evaluation of RF electromagnetic communication in underwater sensor networks," *IEEE Communications Magazine*, vol. 48, no. 12, pp. 143–151, Dec 2010.

[8] X. Che, I. Wells, G. Dickers, and P. Kear, "TDMA frame design for a prototype underwater RF communication network," *Ad Hoc Networks*, vol. 10, no. 3, pp. 317–327, May 2012.

[9] G. Benelli, A. Pozzebon, G. Raguseo, D. Bertoni, and G. Sarti, "An RFID based system for the underwater tracking of pebbles on artificial coarse beaches," in *Third International Conference on Sensor Technologies and Applications*. IEEE, 2009, pp. 294–299.

[10] E. Jimenez, G. Quintana, P. Mena, P. Dorta, I. Perez-Alvarez, S. Zazo, M. Perez, and E. Quevedo, "Investigation on radio wave propagation in shallow seawater: Simulations and measurements," in *2016 IEEE Third Underwater Communications and Networking Conference(UComms)*. IEEE, 2016.

[11] H. Zhang and F. Meng, "Exploiting the skin effect using radio frequency communication in underwater communication," in *International Conference on Industrial Control and Electronics Engineering*. IEEE, 2012, pp. 1150–1153.

[12] A. Pozzebon, "Bringing near field communication under water: short range data exchange in fresh and salt water," in *International EURASIP Workshop on RFID Technology (EURFID)*. IEEE, 2015, pp. 152–156.

[13] A. Abdou, A. Shaw, A. Mason, A. Al-Shamma'a, J. Cullen, and S. Wylie, "Electromagnetic (EM) wave propagation for the development of an underwater wireless sensor network (WSN)," in *SENSORS, 2011 IEEE*. IEEE, 2011, pp. 1571–1574.

[14] H. F. G. Mendez, C. Gac, F. Le Pennec, and C. Person, "High performance underwater UHF radio antenna development," in *OCEANS 2011 IEEE-Spain*. IEEE, 2011.

[15] F. Campagnaro, R. Francescon, F. Guerra, F. Favaro, P. Casari, R. Diamant, and M. Zorzi, "The DESERT underwater framework v2: Improved capabilities and extension tools," in *Proc. Ucomms*, Lerici, Italy, Sep. 2016.

[16] "LoRa Alliance - Homepage," https://lora-alliance.org/, Last time accessed: Apr. 2022.

[17] "Electrical characteristics of the surface of the Earth," Network Working Group, "International telecommunication union (ITU)" 527-6, September 2021.